

# The Properties of Galaxies in Voids

Santiago G. Patiri<sup>1\*</sup>, Francisco Prada<sup>2</sup>, Jon Holtzman<sup>3</sup>, Anatoly Klypin<sup>3</sup> & Juan Betancort-Rijo<sup>1,4</sup>

<sup>1</sup> *Instituto de Astrofísica de Canarias, C/ Via Lactea s/n, Tenerife, E38200, Spain*

<sup>2</sup> *Ramon y Cajal Fellow, Instituto de Astrofísica de Andalucía (CSIC), E-18008, Granada, Spain*

<sup>3</sup> *Astronomy Department, New Mexico State University, Dept. 4500, Las Cruces, NM 88003, USA*

<sup>4</sup> *Facultad de Física, Universidad de La Laguna, Astrofísico Francisco Sanchez, s/n, La Laguna Tenerife, E38200, Spain*

14 June 2018

## ABSTRACT

We present a comparison of the properties of galaxies in the most underdense regions of the Universe, where the galaxy number density is less than 10% of the mean density, with galaxies from more typical regions. We have compiled a sample of galaxies in 46 large nearby voids that were identified using the Sloan Digital Sky Survey DR4, which provides the largest coverage of the sky. We study the  $u - r$  color distribution, morphology, specific star formation rate, and radial number density profiles for a total of 495 galaxies fainter than  $M_r = -20.4 + 5 \log h$  located inside the voids and compare these properties with a control sample of field galaxies. We show that there is an excess of blue galaxies inside the voids. However, inspecting the properties of blue and red galaxies separately, we find that galaxy properties such as color distribution, bulge-to-total ratios, and concentrations are remarkably similar between the void and overall sample. The void galaxies also show the same specific star formation rate at fixed color as the control galaxies. We compare our results with the predictions of cosmological simulations of galaxy formation using the Millennium Run semi-analytic galaxy catalog. We show that the properties of the simulated galaxies in large voids are in reasonably good agreement with those found in similar environments in the real Universe. To summarize, in spite of the fact that galaxies in voids live in the least dense large-scale environment, this environment makes very little impact on properties of galaxies.

**Key words:** cosmology; observations; galaxies: fundamental parameters – galaxies: statistics

## 1 INTRODUCTION

It has been known for many years that the properties of the galaxies depend on their local environments. Dressler (1980) pointed out that the fraction of late-type spirals is larger in regions of lower local density. A similar trend was observed for star formation rates (SFR): star-forming galaxies lie in more underdense regions. On the other hand, the most massive ellipticals and galaxies with low star formation rates reside preferentially in the most dense environments, especially in rich clusters of galaxies (e.g. Postman & Geller 1984; Dressler et al. 2004). Recently, Hogg et al. (2004) show that in all different local environments the bulge-dominated galaxies, defined as those with large Sérsic indices, show

a color-magnitude diagram dominated by red galaxies and that the most luminous galaxies reside preferentially in high-density regions while blue galaxies live mainly in low-density regions.

The  $u - r$  color distribution drawn from the Sloan Digital Sky Survey (SDSS) is well modeled by two Gaussian distributions which can be used to split the samples into a blue and a red galaxy population (see Strateva et al. 2001; Baldry et al. 2004). Although the mean and variance of these two distributions are strong functions of luminosity, or stellar mass (see also Bernardi et al. 2003a; Blanton et al. 2003b; Hogg et al. 2004), there is only a weak dependence of these quantities on the environment (Balogh et al. 2004; Hogg et al. 2004). Nevertheless, the relative fraction of red and blue galaxies strongly depends on local density. At fixed luminosity, the fraction of red galaxies change from 10%-30% in

\* E-mail: spatiri@iac.es

low density environments to about 70% in highest density environments.

Extensive studies on the dependence of galaxy properties with environment has been done for galaxies lying in high-density regions such as groups and clusters and its comparison with the field (see Dressler et al. 2004, and references therein). More recently, thanks to the advent of large redshift surveys, it has become possible to study the properties of galaxies lying in the most underdense regions of the Universe.

Grogin & Geller (2000) selected a sample of galaxies from the CfA redshift survey that are located in regions with galaxy number density contrast ( $\delta_{gal} = (\bar{n}_v/\bar{n}) - 1$ , where  $\bar{n}_v$  is the number density of galaxies in the scale of interest and  $\bar{n}$  is the mean number density of galaxies in the sample) of  $\leq -0.5$ . They studied a total of 149 galaxies in these environments, finding these galaxies to be bluer than those in the field and also showed that a significant fraction of them were late type spirals. Recently, Rojas et al. (2004, 2005) studied a sample of  $\sim 1200$  galaxies, extracted from the SDSS SAMPLE10 (about 1.5 times the SDSS DR1), located in regions with  $\delta_{gal} \leq -0.5$ . They also find that void galaxies are bluer on average than the general galaxy population and that they have a higher specific star formation rate. They claim that this difference is not just caused by the morphology-density relation; they find that late-type galaxies (as defined by a global Sersic index fit) in voids differ from those outside of voids. Croton et al. (2005), using the 2dFGRS, also showed that the galaxy population in underdense regions differs from that in the field. They found that a late-type population dominates the low density regions, while cluster regions have a relative excess of very bright early-type galaxies.

The study of the properties of galaxies in large underdense regions can provide strong constraints to the galaxy formation processes. Benson et al. (2003) used semi-analytic models in order to study the predictions concerning galaxies within voids. Although the resolution they used in their simulations were not sufficiently high to take full description of the properties of galaxies in underdense regions, they found that the galaxy population in these regions is bluer than the field. Also, they found that the specific star formation rate is higher in the central regions of the voids than the boundaries. Today, with the advent of higher resolution simulations and the improvements in the prescriptions for galaxy formation it is possible to make more robust predictions.

In this paper, we use the latest public data release of the SDSS (Data Release 4) in order to study statistically the properties of galaxies lying in the most underdense regions of the universe, those with  $\delta_{gal}$  about -0.9. We specifically take advantage of a large contiguous region spanned by the DR4 in order to find for the first time large voids that have previously been impossible to identify. In addition, we compare our results with the latest predictions from the semi-analytic models, using the recently released Millennium Run galaxy catalog (Springel et al. 2005; Croton et al. 2005). In order to make this comparison, we analyze the galaxies found in voids in this mock catalog.

The work is organized as follows. In Section 2 we describe the observational data set and the method for searching for large voids. In Section 3 we present our results on the properties of galaxies in voids. In Section 4 we compare

our results with the predictions of the recently released Millennium Run galaxy catalog (Springel et al. 2005; Croton et al. 2005). Finally, in Section 5, we present our conclusions.

Throughout the paper we assume a  $\Lambda$ CDM cosmology with parameters  $\Omega_m = 0.3$ ,  $\Omega_\Lambda = 0.7$  and  $H_0 = 100 h \text{ km/s/Mpc}$ .

## 2 SEARCHING FOR VOIDS IN THE SDSS DR4

The SDSS is the largest photometric and spectroscopic survey to date; the completed survey will cover approximately 8000 square deg. CCD imaging is done in five colors and spectroscopic follow-up of galaxies is performed down to  $r=17.77$  mag; see York et al. (2000) and Stoughton et al. (2002) for a complete overview of the survey. The details of selection function for galaxy spectroscopy and spectroscopic tiling can be found in Strauss et al. (2002) and Blanton et al. (2003a). A thorough analysis of systematic uncertainties in the galaxy samples is described in Scranton et al. (2002).

Although the SDSS spectroscopic sample is magnitude limited, there is some incompleteness due to missing nearby bright galaxies ( $r < 15.5$ ) to avoid fiber saturation, and missing galaxies from the need to avoid fiber collisions (7%; Blanton et al. 2003a), redshift failures (<1%) and some galaxies ( $\sim 1\%$ ) blotted out by bright Galactic stars. This incompleteness may cause a slight overestimation in the final underdensities.

In the present work we use the latest public version of the survey, the SDSS DR4. This release has a total of 410,939 galaxy spectra distributed in several regions or strips covering a region of about 4,800 sq. degrees on the sky. The galaxy sample is distributed in three regions. The first one is located in the North Galactic Cap (NGC) and the other two are in the South Galactic Cap (SGC), near the celestial equator. Although the geometry of these regions is rather complex, we were able to select a geometrically contiguous region from the NGC, which we refer to as the North Strip (NS). The North Strip covers an area of  $\sim 2,000$  sq. degrees on the sky going from  $117^\circ < \text{RA} < 200^\circ$  and  $+20^\circ < \text{DEC} < +70^\circ$ . The large declination range of this region allows us to search for large nearby voids with high underdensities.

We define voids as the maximal non-overlapping spheres empty of galaxies with luminosity above a given value. For example, we could define voids as maximal spheres empty of Milky Way-size galaxies. Although the voids are empty of these galaxies, they can have fainter galaxies inside (see Patiri et al. 2006b for a full discussion on different void definitions and uses). Note that as we are interested in studying the galaxies located in the most underdense regions of the universe we search for very large voids, i.e. those with a radius much larger than the mean distance between galaxies.

To select galaxies which define our voids, we use SDSS  $r$ -band magnitudes. Absolute magnitudes are computed from the extinction-corrected apparent magnitudes assuming a  $\Lambda$ CDM cosmology and taking into account the  $k$ -correction using the prescription developed by Blanton et al. (2003b).

The SDSS DR4 is a flux-limited survey. So, there is a decrease of observed galaxies with redshift. In order to search for large nearby voids, we construct from the NS sample a volume-limited galaxy sample with  $z_{max} = 0.085$  using red-

shifts with confidence level greater than 0.95, corresponding to a volume out to a distance of  $250h^{-1}\text{Mpc}$ . Within this volume, the spectroscopic survey is complete to a limiting absolute magnitude of  $M_r^{\text{lim}} = -19.4 + 5\log h$ . The total volume of our sample is  $2.31 \times 10^6 h^{-1}\text{Mpc}^3$  with a total of 27046 galaxies.

We search for large voids in our volume-limited galaxy sample using the *HB void finder* (Patiri et al. 2006b). The *HB Void Finder* is conceptually simple, as it searches for the maximal non-overlapping spheres with radius *larger* than a given value that are empty of galaxies brighter than some specified brightness. This code is designed to be accurate and computationally efficient in finding the largest voids in a galaxy sample. To search for voids, the code first generates a sphere of fixed radius randomly located within the galaxy sample. We check whether this sphere is empty of bright galaxies. If so, we increase the size of the sphere until its surface reaches the four nearest galaxies. If this sphere does not overlap another one, we define it as a void. If it does overlap, the larger sphere is taken to be the void. To assure that the full sphere is entirely inside the galaxy sample, we put artificial guard “luminous galaxies” on the borders of the sample. For a full description of the algorithm see Patiri et al. (2006b).

In the present paper we search for voids defined by absence of galaxies brighter than  $M_r = -20.4 + 5\log h$ . The mean number density of these galaxies is  $4.2 \times 10^{-3} h^{-1}\text{Mpc}^{-3}$ , with a mean distance between the galaxies of  $\sim 6.2h^{-1}\text{Mpc}$ . Since we are interested in large voids, we start the void finder with a minimum radius of  $10.0h^{-1}\text{Mpc}$ . Note, that a randomly placed sphere with a radius of  $14.0h^{-1}\text{Mpc}$  would contain typically 50 galaxies of those defining the voids (i.e. galaxies brighter than  $M_r = -20.4 + 5\log h$ ).

Using these definitions, we find in our volume-limited sample a total of 46 voids with radius larger than  $10.0h^{-1}\text{Mpc}^1$ . The largest void has a radius of  $17.3h^{-1}\text{Mpc}$ . In Figure 1 we show one of our large voids in the SDSS NS flux-limited sample and its surrounding large scale structure. The big dots denote the galaxies defining the voids (brighter than  $M_r = -20.4 + 5\log h$ ); small dots are fainter galaxies. In the inset we magnify the void region. Note that although the void is empty of bright galaxies, it is populated by fainter galaxies. These faint galaxies are not randomly distributed: they are arranged in small groups and filaments. This distribution resembles the large scale structure of the Universe. Very similar results were found in the high resolution N-body simulations of voids defined by dark matter halos (Gottlober et al. 2003).

As we mentioned above, the extensive coverage of the most recent SDSS data release enables the search for such large empty voids for the first time. In previous studies of “void galaxies” in SDSS (Rojas et al. 2004, 2005), the data set was much more limited. As a result, “void galaxies” were selected by a nearest-neighbor analysis by looking for galaxies (within a specified magnitude range) whose third nearest neighbor was at distance larger than  $7h^{-1}\text{Mpc}$ . This method includes galaxies in voids much smaller than we

consider here, and also occasionally allows galaxies in low-density filaments to be counted as void galaxies. Although this procedure yields a very large sample of galaxies, the environment where galaxies are located is not so underdense. Our current sample represents the galaxies in the largest and emptiest voids, and, thus, perhaps is expected to provide the strongest constraints on how void galaxies compare to galaxies in the general population.

### 3 THE PHYSICAL PROPERTIES OF GALAXIES IN LARGE VOIDS

In our sample of 46 nearby voids larger than  $10.0h^{-1}\text{Mpc}$  we find a total of 495 galaxies fainter than  $M_r = -20.4 + 5\log h$ , and brighter than our limiting magnitude of  $M_r = -19.4 + 5\log h$ . To determine whether the properties of these galaxies differ systematically from those outside of voids, using our volume-limited sample we construct a control sample of field galaxies by taking galaxies which happen to be inside randomly selected spheres of radius  $13h^{-1}\text{Mpc}$ . We then take all galaxies in the same luminosity range as our void galaxies. Using the void and the control samples, we can compare color distributions, morphology, and specific star formation rates. We also investigate the number density profiles of galaxies within voids. Finally, we compare the observed properties of our void galaxies with simulated galaxies.

#### 3.1 Galaxy number density profiles

We define the number density profile of galaxies in voids as:

$$1 + \delta_{gal}(r) = \frac{n_{void}(r)}{n}, \quad (1)$$

where  $n_{void}(r)$  is the mean number density of galaxies averaged over all our voids at a distance  $r$  from the center of the void and  $n$  is the mean number density of galaxies in our volume-limited sample for the same magnitude bin.

In the bottom panel of Figure 2 we show the number density profile of faint galaxies in voids with radii between  $10h^{-1}\text{Mpc}$  and  $13h^{-1}\text{Mpc}$  as a function of distance from the void center (normalized to the void radius,  $R_{void}$ ). The solid line in Figure 2 shows the  $1 + \delta_{gal}$  profile. We can see that the number density profile of galaxies inside voids is quite flat. The mean (enclosed) number density of galaxies at  $R_{void}$  is 10% that of the field. Beyond  $R_{void}$  the local number density profile shows a remarkably steep increase, reaching a local density of 90% of the mean density at  $1.4 R_{void}$ .

In the top panel of Figure 2 we show the number density profile of galaxies for voids with radius larger than  $13h^{-1}\text{Mpc}$ . We can see a similar behavior shown in the smaller voids. However, larger voids have a flatter profile and the increase with radius is not so sharp. At distance  $1.4R_{void}$ , the density is about 60% of the mean density. Note that we do not see a spike in the number density around  $R_{void}$  as predicted by numerical and analytical estimates of voids defined by dark matter halos (see e.g., Colberg et al. 2005; Patiri et al. 2006a). A possible reason for the absence of the spike could be due to redshift distortions, which smooth out the spike. Spatial bias may also be involved.

Error bars in the number density profiles have been calculated using the Millennium Run galaxy catalog, which is

<sup>1</sup> The full list of coordinates and sizes of these voids are available upon request

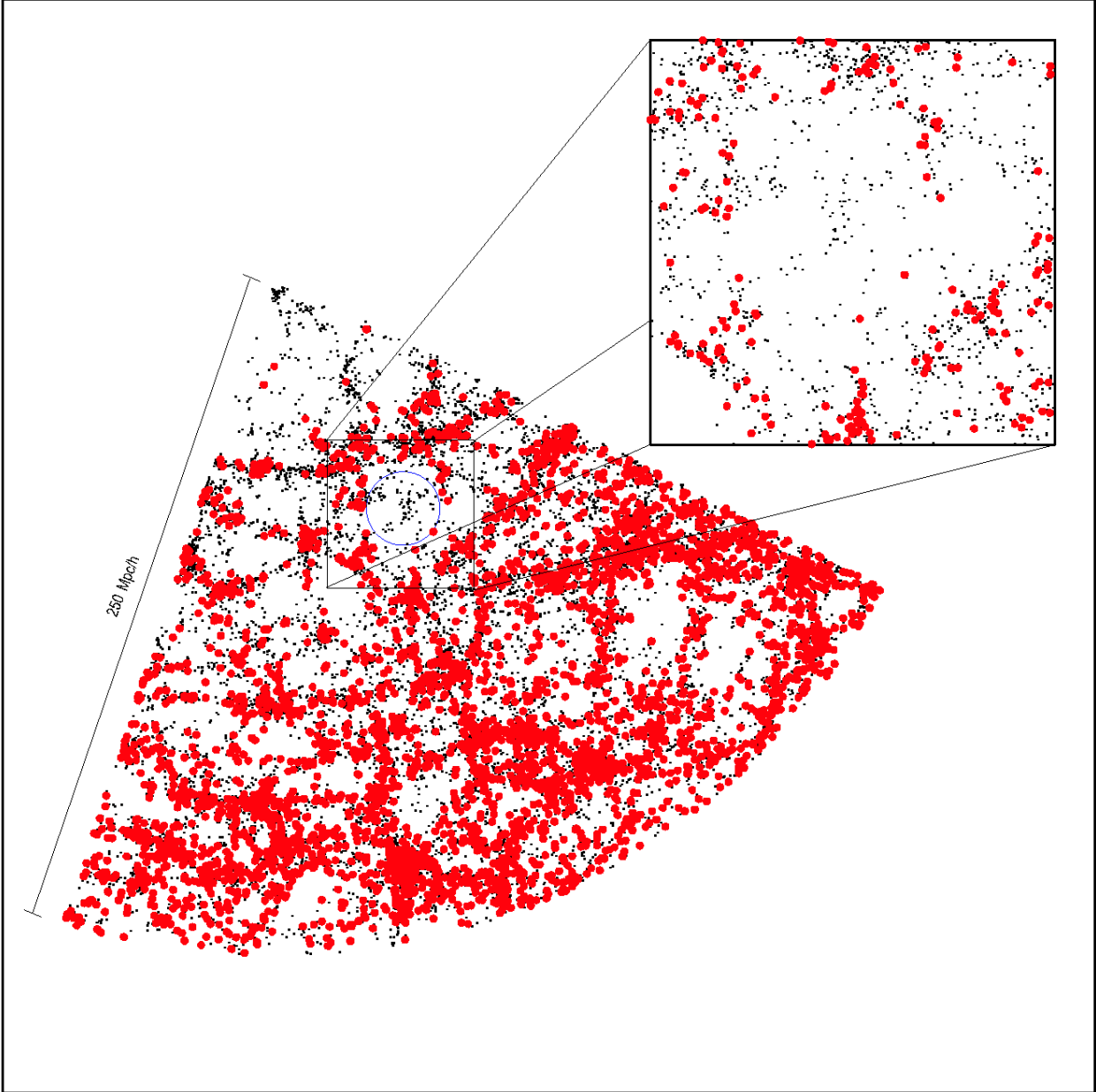


**Figure 1.** A slab of  $9h^{-1}\text{Mpc}$  of our SDSS NS flux-limited galaxy sample. We show one of our large voids (circle). This void has a radius of  $13h^{-1}\text{Mpc}$  and it is defined by galaxies brighter than  $M_r = -20.4 + 5\log h$  (big dots). We also plot fainter galaxies (small dots). The inset shows a zoom of the void region of size  $60h^{-1}\text{Mpc}$ . Note that the faint galaxies populating the voids are not randomly distributed: they are clustered in small groups and filaments in a similar way to that of the brighter galaxies.

discussed in more detail in Section 4. Using the simulated catalog we can estimate the deviations of the profiles that includes the sampling error, as well as cosmic variance. In order to compute the error bars, we use a list of 2000 voids found in the entire catalog (see Section 4.1). From this list, we randomly select a set of 50 samples each containing 46 voids as in our SDSS sample. For each sample we obtain the number density profile averaging over the 46 voids. We find comparable number of galaxies per void. So, we end up with a sample of 50 profiles and we estimate the rms deviation in each radial bin over the ensemble of the 50 profiles.

In Figure 3, we show the profiles for blue (solid line) and red galaxies (dashed line) separately, for the smaller

voids (bottom) and larger voids (top). There are galaxies of both populations throughout the voids; both red and blue galaxies increase rapidly in density at the edges of the voids.

### 3.2 Color distributions

In Figure 4 we plot the  $u-r$  color distribution of the galaxies in our void sample (black points). We also show the color distribution of galaxies in the control sample (full line). The error bars ( $\Delta F$ ) are derived using the binomial distribution:

$$\Delta F = \frac{\Delta n}{N}; \quad \Delta n = \sqrt{n(1-F)}, \quad (2)$$

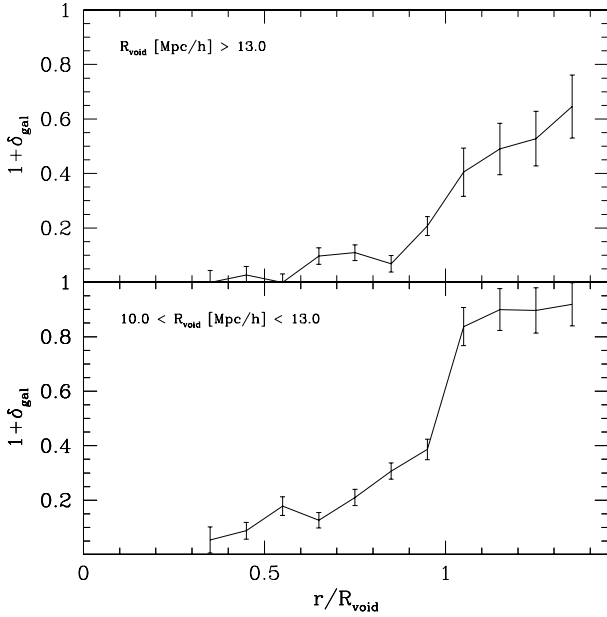


**Figure 2.** Top panel: number density profile ( $1 + \delta_{gal}$ ) for galaxies in voids with radius larger than  $13h^{-1}$ Mpc found in the SDSS NS sample as a function of the void radius. Bottom panel: number density profile for galaxies in voids with radius between  $10h^{-1}$ Mpc and  $13h^{-1}$ Mpc.

where  $F$  is the galaxy number fraction for each  $u - r$  color bin.  $n$  is the number of galaxies in each bin, and  $N$  is the total number of galaxies found in our voids.

We clearly see that both  $u - r$  galaxy color distributions are bimodal. There is an excess of blue galaxies in the voids relative to the control sample in this luminosity bin ( $-19.4 > M_r - 5 \log h > -20.4$ ). This behavior has been shown previously for galaxies in local underdense regions with  $\delta_{gal} < -0.6$  (e.g., Balogh et al. 2004; Rojas et al. 2004).

However, if we look at the blue ( $u - r < 2.0$ ) and red ( $u - r > 2.0$ ) galaxy populations separately, we find a mean  $\langle u - r \rangle = 1.61$  for the blue population in our voids, while for the blue population in the control sample the mean color is  $\langle u - r \rangle = 1.62$ . For red galaxies we get  $\langle u - r \rangle = 2.37$  and  $\langle u - r \rangle = 2.4$  for void and field galaxies, respectively. The mean colors of red and blue galaxies separately are essentially identical inside voids and in the field. Figure 5 shows the normalized color distributions of blue and red galaxies separately; it is clear that the void and field distributions for galaxies of the same color are practically indistinguishable.

### 3.3 Morphology

While color is to some extent likely to be related to morphology, our sample is sufficiently nearby that we are able to quantify the morphology of galaxies directly from the SDSS imaging, and to compare the morphology of void and control galaxies.

Figure 6 (upper panels) shows the distribution of concentrations of the void (histograms) and control (curves) samples; concentration is defined as  $c \equiv r_{90}/r_{50}$ , where  $r_{90}$  and  $r_{50}$  are the radii enclosing 90 and 50% of the Pet-

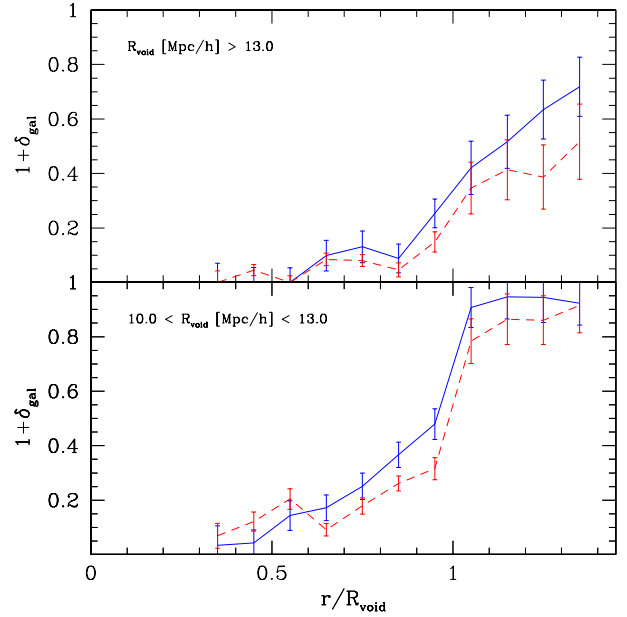


**Figure 3.** Top panel: number density profile ( $1 + \delta_{gal}$ ) for red galaxies (dashed line) and blue galaxies (full line) in voids with radius larger than  $13h^{-1}$ Mpc. Bottom panel: the same profiles for voids with radii between  $10h^{-1}$ Mpc and  $13h^{-1}$ Mpc.

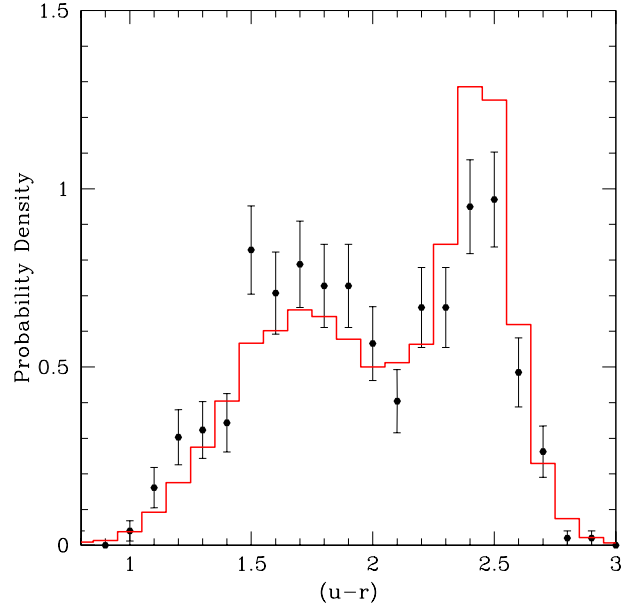


**Figure 4.**  $u - r$  color distribution for void galaxies found in the SDSS NS sample in the  $-19.4 > M_r - 5 \log h > -20.4$  magnitude range (black dots). The full line gives the  $u - r$  color distribution for galaxies in the control sample in the same magnitude bin.

rosian flux respectively, as measured by the SDSS PHOTO pipeline. The comparison between void and control samples is done for the entire samples (left panel), as well as separately for the blue (center) and red (right) galaxies. It is apparent that there are no visible differences in the distribution of concentrations, especially within the subsamples

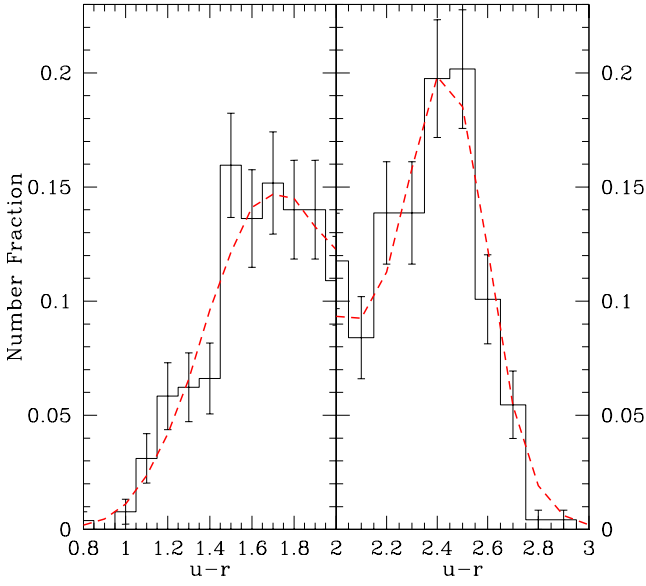


**Figure 5.** Left panel:  $u-r$  color distribution for galaxies lying in voids (full line) and field galaxies (short dashed line) normalized to the blue population. Right panel: the same but for the red population. Note that the mean and variance of both populations are very similar for galaxies in voids and in the field.

selected by color. Since blue galaxies have lower concentrations than red galaxies, and since we have shown that there are a larger fraction of blue galaxies in voids, the concentrations for the full samples are shifted to slightly smaller values in voids.

To get additional sensitivity to morphology, we perform bulge to disk decomposition on all of the galaxies in the void and control samples. This is done using a nonlinear least squares fit to the data with a galaxy model that includes an inclined, circular, exponential disk and a flattened Sersic bulge; additional details are given in MacArthur et al. (2003). To do the fit, a one-dimensional profile is constructed from the data by fitting elliptical isophotes to the image. From the 1D profile, an exponential disk model was fit from  $r_{50} < r < r_{pet}$ , and a deVaucouleurs (Sersic  $n = 4$ ) profile was fit to  $r < r_{50}$ . The 1D fits are done assuming a Gaussian PSF, where the FWHM was measured from the SDSS PSF. These initial estimates are used as a starting guess to fit a composite disk plus bulge model to the entire 1D profile out to  $r_{pet}$ , fixing the bulge to be a deVaucouleurs bulge. The resulting decomposition is then used as a starting guess for a 2D fit on the SDSS data. The 2D fits are done using the 2D PSF determined by the SDSS PHOTO pipeline. Separate fits are done fixing the Sersic index at  $n = 1, 2, 3, 4$  separately. Finally, a fit is done allowing for  $n$  to float, using the best fit model of the fixed Sersic fits as a starting guess. We note that getting a unique fit for Sersic index is difficult for most of the galaxies due to their limited angular extent; the derived Sersic index has a strong covariance with the bulge effective radius. We compute the bulge/total light ratio from the fits, where  $B/T$  is computed within the Petrosian radius; with this definition, the  $B/T$

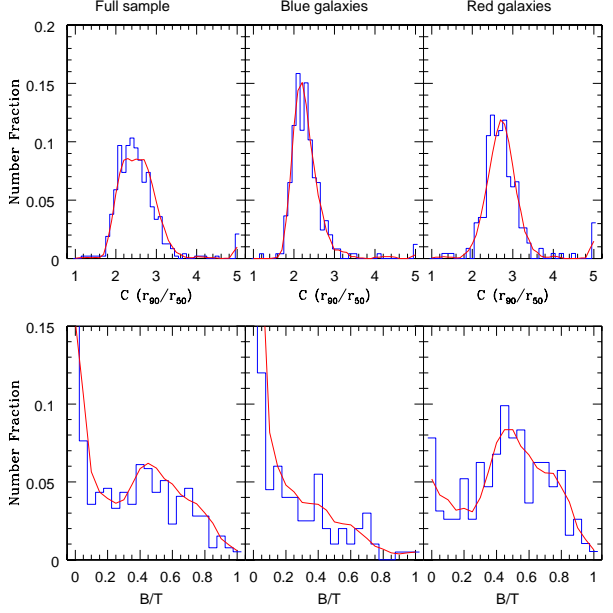


**Figure 6.** Upper panels: Distribution of concentrations of the void (histograms) and field (curves) galaxies. In the three panels we show the distributions for all the galaxies (left), for the blue population (center) and red population (right). Bottom panels: Distribution of Bulge-to-Total ratios for galaxies found in the SDSS. The histograms denote galaxies in the voids and the curves are for the galaxies in the field. Left panel shows all the galaxies, center panel only blue galaxies, and right panel only red galaxies.

ratio is rather insensitive to different combinations of Sersic index and bulge effective radius.

In the bottom panels of figure 6, we show the distribution of  $B/T$  ratios for the floating  $n$  fit. Because of the insensitivity of  $B/T$  to the Sersic index, the distributions for the fixed and floating Sersic index are very similar. As with the concentrations, the left panel shows the distributions for the entire void and control samples, the center panel the distributions for the blue galaxies, and the right panel the distributions for the red galaxies. In this figure, we can see that there are a significant number of galaxies with  $B/T = 0$ . These result for any galaxy for which an inward extrapolation of an exponential fit to the outer regions matches or over-predicts the flux in the central region. While pure disk galaxies with no bulge fall into this category, so do spheroidal galaxies with an exponential profile (not necessarily unexpected for the lower luminosity galaxies in our sample), as do disk galaxies with profiles that are not fully exponential, e.g. galaxies with an inner flattening or truncation. As a result, the  $B/T = 0$  bin is rather heterogeneous. Aside from this bin, the distributions of  $B/T$  ratios are quite similar between void and field galaxies. Although the  $B/T$  ratios are clearly different for the blue and red galaxies, the relative change in the ratio of blue/red galaxies from field to void is subtle enough that it is difficult to see the effect in the overall distribution of  $B/T$ .

Figure 7 gives distribution of several morphological properties of galaxies as function of color of the galaxies. There are no apparent differences between void galaxies and the control sample in any of the presented properties.

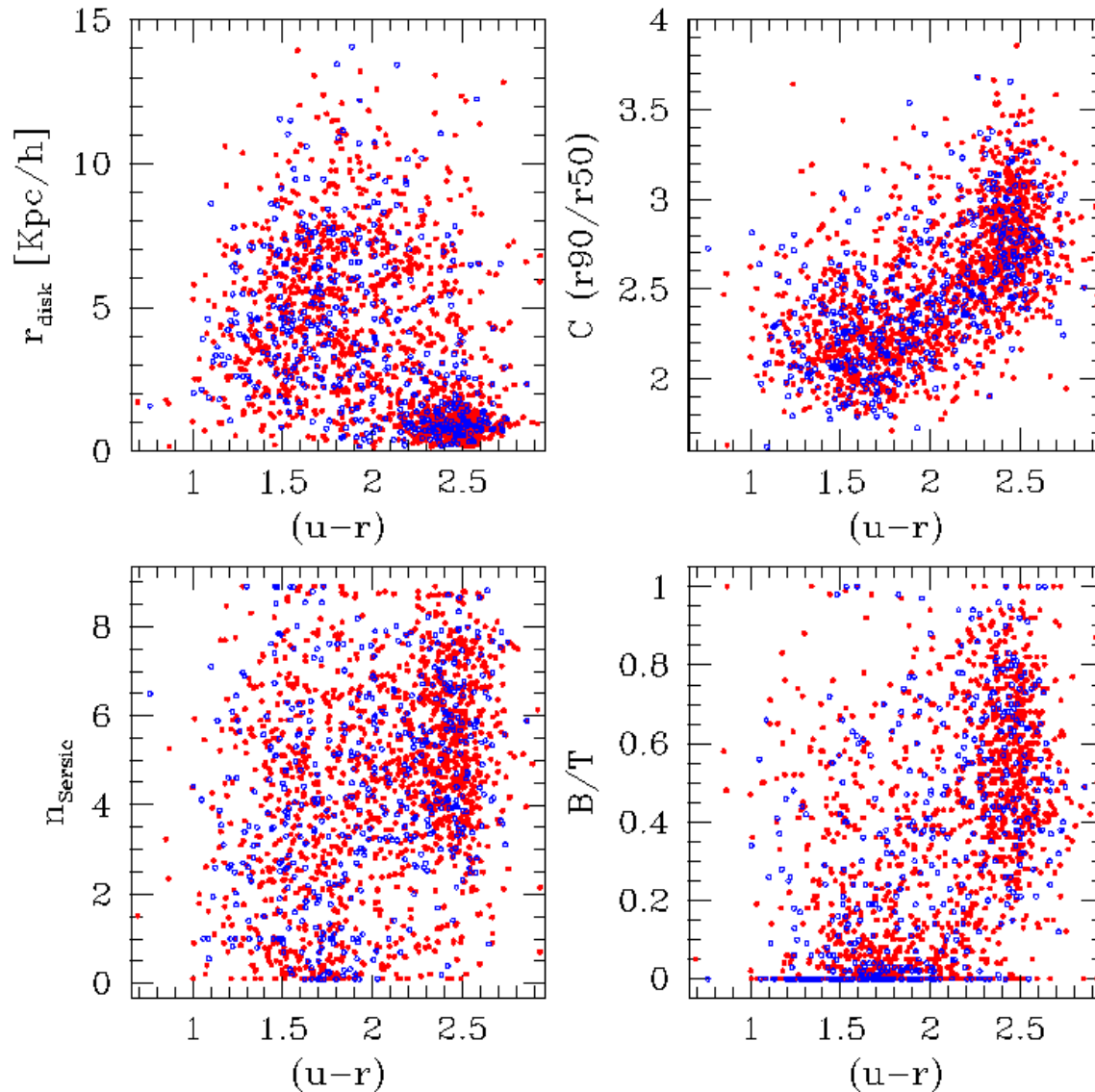


**Figure 7.** Morphological properties of galaxies vs.  $u - r$  color for galaxies found in our SDSS sample. The open circles denote galaxies in voids and the full circles are the control galaxies. Upper Left: Disk scale length. Upper Right: Concentration. Bottom Left: The Sersic parameter ( $n$ ) obtained for the bulge. Bottom right: Bulge-to-Total luminosity ratios.

### 3.4 Specific star formation rates

The specific star formation rate is defined as the star formation rate per unit of stellar mass ( $M_*$ ). The SFRs and stellar mass data for the galaxies in the SDSS DR4 have been recently made publicly available<sup>2</sup> (Kauffmann et al. 2003; Brinchmann et al. 2004). The SFRs were obtained by comparing the width of the emission lines with the continuum properties of the galaxies: a method was developed for aperture correction using the imaging available from the SDSS and have shown that the method takes out essentially

all aperture bias in the SFR estimates, allowing an accurate estimate of the total SFRs in galaxies. (see Brinchmann et al. 2004 for details). Stellar masses were estimated using the spectroscopic information and broad-band photometry available in the SDSS (Kauffmann et al. 2003). The procedure also provides an estimate of the extinction.

Figure 8 shows the specific star formation rate of our void galaxies as a function of  $u - r$  color (open circles); data for the control sample are also shown (full circles). There is a strong correlation between galaxy color and specific SFR. Although there are relatively more blue galaxies (with higher specific SFR) in voids, the void galaxies appear indistinguishable from the galaxies in the control sample at fixed galaxy color. This suggests a common star formation his-

<sup>2</sup> The SFR and  $M_*$  for the SDSS DR4 galaxies can be downloaded from <http://www.mpa-garching.mpg.de/SDSS/DR4/>

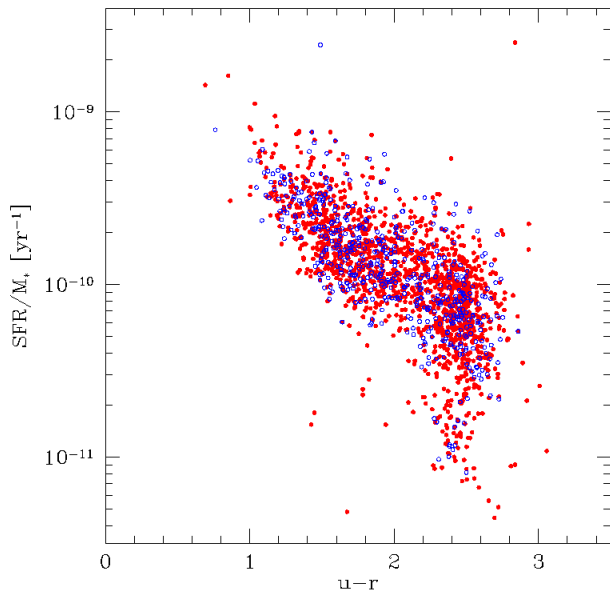


**Figure 8.** The specific star formation rate of galaxies lying in our large voids in the SDSS NS sample as a function of  $u-r$  color (open circles). The full circles show the same for the galaxies in the field. There is not a significant difference for galaxies of fixed color between voids and field.

tory inside and outside of voids for galaxies with the same current star formation rate.

## 4 COMPARISON WITH THE MILLENNIUM RUN

### 4.1 The galaxy catalog

The Millennium Run is a large cosmological numerical simulation of  $2160^3$  dark matter particles in a box of  $500h^{-1}\text{Mpc}$  on a side; for a full description see Springel et al. (2005b). The formation of galaxies is tracked from the dark matter simulation using a semi-analytic model to follow gas, stars and supermassive black hole processes within the merger history trees of dark matter halos and their substructures. The modeling assumptions and parameters are adjusted by trial and error in order to fit the observed properties of low redshift galaxies, primarily their joint luminosity-color distribution and their distributions of morphology, gas content and central black hole mass.

The public available Millennium Run galaxy catalog<sup>3</sup> (Springel et al. 2005; Croton et al. 2005) contains a total of about 9 million galaxies in the full simulation box. For each galaxy, the catalog provides the position and velocity, the total and bulge galaxy magnitudes in 5 bands (SDSS ugriz), the total and bulge stellar mass, cold, hot and ejected gas mass, the black hole mass, and the star formation rate.

We use these data to study the properties of galaxies in the most underdense regions of the simulated catalog.

<sup>3</sup> It can be downloaded from <http://www.mpa-garching.mpg.de/galform/agnpaper/>

This offers an unique opportunity to compare with the results that we find in the SDSS. We make the same analysis for the Millennium galaxy catalog as for our volume-limited galaxy sample drawn from the SDSS. To this end, the first step is to search for voids. We divide the entire Millennium box in several smaller boxes of comparable volume to that of our SDSS NS galaxy sample; specifically, we divide the  $500h^{-1}\text{Mpc}$  box into 27 small boxes with  $166.67h^{-1}\text{Mpc}$  on a side. In order to make a direct comparison with observations, we transformed the real space catalogs produced for the small boxes to redshift space using the real coordinates and the peculiar velocities. Then, we search for voids in each small box with the same parameters that we use for the SDSS analysis, i.e. we searched for voids defined to be empty of galaxies brighter than  $M_r = -20.4 + 5\log h$ . The mean number density of these galaxies is  $4.3 \times 10^{-3}h^{-1}\text{Mpc}^{-3}$ , very similar to that found in our SDSS NS sample. On average over the small Millennium Run boxes, we have found 78 voids larger than  $10.0h^{-1}\text{Mpc}$ . This number is compatible with the number of voids found in the SDSS taking in account that the small boxes in Millennium have twice the volume than our observational sample.

### 4.2 Properties of the Millennium Run galaxies

We study the properties of the fainter galaxies lying in these voids down to  $M_R = -19.4 + 5\log h$  as we did in the SDSS. We find on average  $\sim 1000$  galaxies in the voids for each box, which again is compatible with number of galaxies found in the SDSS.

In Figure 9 we show the  $u-r$  color distribution of galaxies lying in these high underdense regions found in all boxes (black dots). The error bars are the standard deviation derived from the ensemble of the 27 small boxes. We also show the comparison for galaxies in the field for the same magnitude interval (full line). In the voids, there is clearly a larger ratio of blue to red galaxies, as we see in the observations. However, the difference between voids and field is clearly more pronounced in the simulations than in the real data. The simulations have significantly more blue galaxies than red galaxies in the voids, while the observations show roughly comparable numbers. If we divide the galaxies into blue and red populations, we find that the mean and variance of the blue population is the same in voids and in the field, as we see in the observations (see fig.10). Red galaxies in the simulations appear to differ slightly between voids and field, which is somewhat different from what we see in the observations.

In Figure 11 we show the number density profile for galaxies in voids with radius larger than  $13h^{-1}\text{Mpc}$  (top panel) and with radius between  $10h^{-1}\text{Mpc}$  and  $13h^{-1}\text{Mpc}$  (bottom panel) as a function of the normalized void radius (dashed line). As a comparison, we also show the same profiles found in the SDSS sample (full lines). In Figure 12 we plot the density profiles separately for both blue and red galaxies, as we did for the observed sample. The profiles from the simulations are similar to those of the observed galaxies.

In Figure 13 we present the specific SFR as a function of  $u-r$  color for galaxies within the large voids in the Millennium Run. This agrees well with that obtained for galaxies in



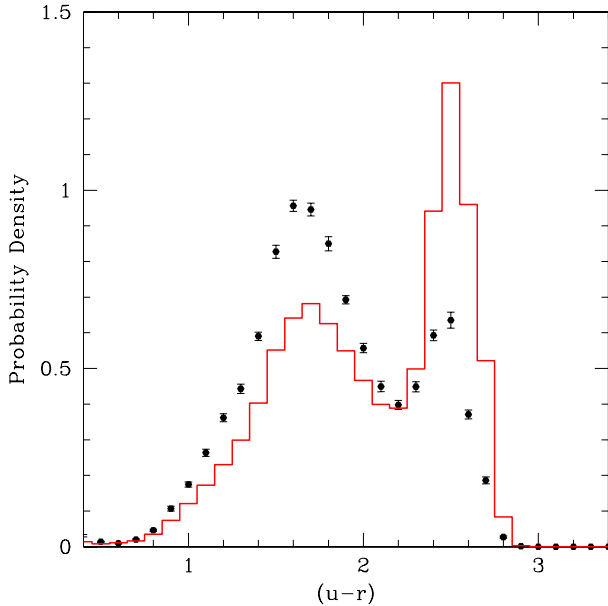


**Figure 9.**  $u - r$  color distribution for galaxies with  $-19.4 > M_r - 5 \log h > -20.4$  lying in large voids found in the Millennium Run (black dots). The color distribution for the galaxies in the field is also shown for comparison (full line).

our observed sample, with comparable star formation rates at fixed color for void and field galaxies.

We use the bulge and total magnitudes in the Millennium Run galaxy catalog to compute the Bulge-to-Total luminosity ratio as a function of the  $u - r$  color for the galaxies inside the large voids (see Figure 14). One can see that blue galaxies are disk-dominated while red galaxies are bulge-dominated. The B/T ratios of very red galaxies (those with  $u - r > 2.5$ ) suggest that these galaxies are ellipticals. The relation between morphology and color appears to be the same in void galaxies as in field galaxies, although the relative number of galaxies as a function of morphology or color differs. To see this more patent, we show in Figure 15 the histograms of  $B/T$  ratios for both void and field galaxies for the populations all together (left panel), for the blue population (central panel) and red population (right panel)

## 5 DISCUSSION AND CONCLUSIONS

We use the SDSS Data Release 4 to study the properties of galaxies lying in the most underdense regions of the universe. We search for nearby ( $z \leq 0.085$ ) large voids with radius larger than  $10.0h^{-1}\text{Mpc}$  in the SDSS North Strip. In total, we find 46 voids larger than  $10.0h^{-1}\text{Mpc}$  with average underdensities  $\delta_{gal} \sim -0.87$ . We study the  $u - r$  color distributions, the qualitative morphology, and the specific star formation rate ( $\text{SFR}/M_*$ ) for a total of 495 galaxies with  $-19.4 + 5 \log h > M_r > -20.4 + 5 \log h$  lying in these voids, and compare these properties with a control sample taken randomly from the SDSS volume. It is important to realize that we do not deal with luminous galaxies here, since by definition, our voids have no luminous galaxies.

Galaxies in voids are not distributed randomly through-

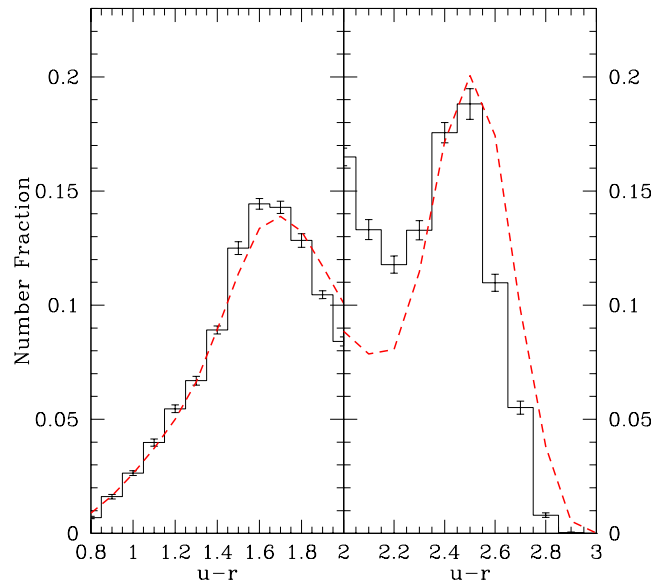


**Figure 10.** Left Panel:  $u - r$  color distribution for simulated blue galaxies lying in voids (full line) and field galaxies (short dashed line). Right Panel: the color distribution of the red population. Here, we can see that red population in voids is shifted compared with the field.

out the void. Typically, they are found in filaments. In addition, the density increases toward the void walls. As a result, although the average galaxy density is very low in the voids, it is not necessarily as low *locally* compared with galaxies outside voids. The number density profiles for the largest voids (those larger than  $13h^{-1}\text{Mpc}$ ) are flat in the inner part of voids and increase rapidly as we go to outer parts, reaching about 60% of the field density at  $1.4$  void radius. The blue and red galaxies have similar profiles. For smaller voids with radii between  $10$  and  $13h^{-1}\text{Mpc}$ , the profiles are flat in the inner half of the voids and rise to the mean density at  $1.2$  void radii. Recent results on the radial profiles of voids defined by dark matter halos (Colberg et al. 2005; Patiri et al. 2006a) show similar trends in the inner parts of voids, but suggest that the density should increase suddenly just beyond  $1 R_{void}$  to form a prominent spike, after which the density declines and reaches the mean density at about  $1.6R_{void}$ . This effect might be due to crossing of spherical shells in the edges of voids. However, we do not see this spike in our observations.

The  $u - r$  color distribution in our luminosity range is clearly bimodal in both the void and control samples. The fraction of blue galaxies, however, is significantly larger in the voids, leading to a galaxy population that is overall bluer. However, the effect does not appear to be as large as for samples that select environment on a smaller scale (e.g., Balogh et al 2004). For example, in the same magnitude range, Balogh et al. (2004) find significantly more blue than red galaxies in their lower local density bins, while we find comparable numbers of blue and red galaxies in our large voids. It is impossible for us to define local density as in Balogh et al. (2004), because their density estimator is based on the proximity of galaxies with  $M_r < -20$ , of which there

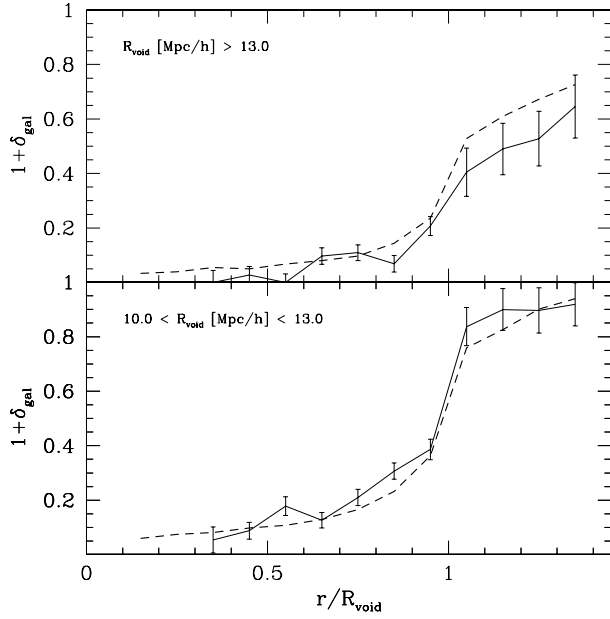


**Figure 11.** Comparison between the number density profiles for voids found in the Millennium Run (dashed line) and SDSS (full line). Top panel: profiles for voids larger than  $13h^{-1}\text{Mpc}$ . Bottom panel: for voids with radius between  $10h^{-1}\text{Mpc}$  and  $13h^{-1}\text{Mpc}$

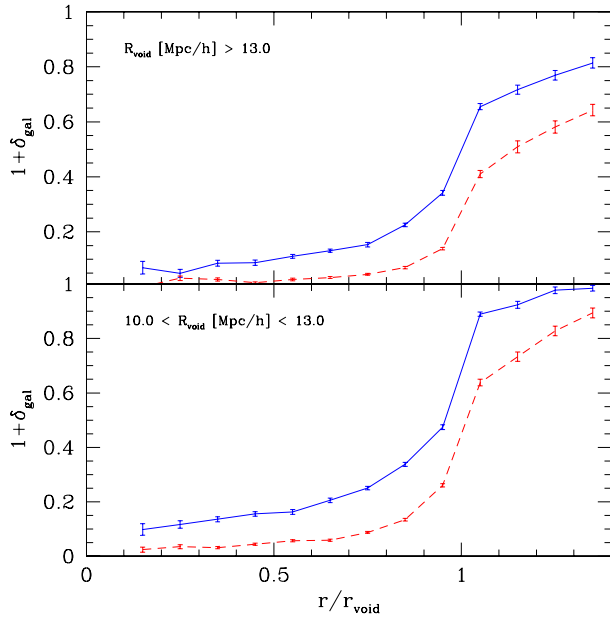


**Figure 12.** Top panel: The local number density profile for red galaxies (dashed line) and blue galaxies (full line) as a function of the normalized void radius for voids with radius larger than  $13h^{-1}\text{Mpc}$  found in the Millennium Run galaxy catalog. Bottom panel: the same profiles but for voids with radius between  $10h^{-1}\text{Mpc}$  and  $13h^{-1}\text{Mpc}$ .

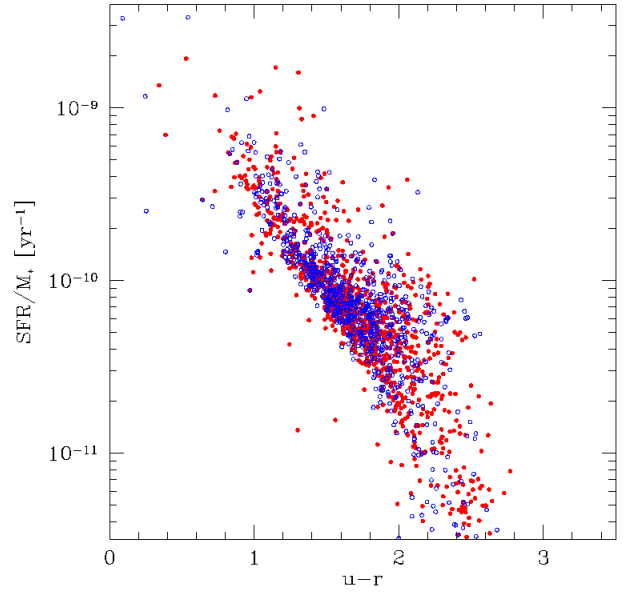


**Figure 13.** Specific Star Formation Rate as a function of  $u - r$  color for the simulated galaxies. Open circles denote galaxies in voids while filled circles are galaxies in the field.

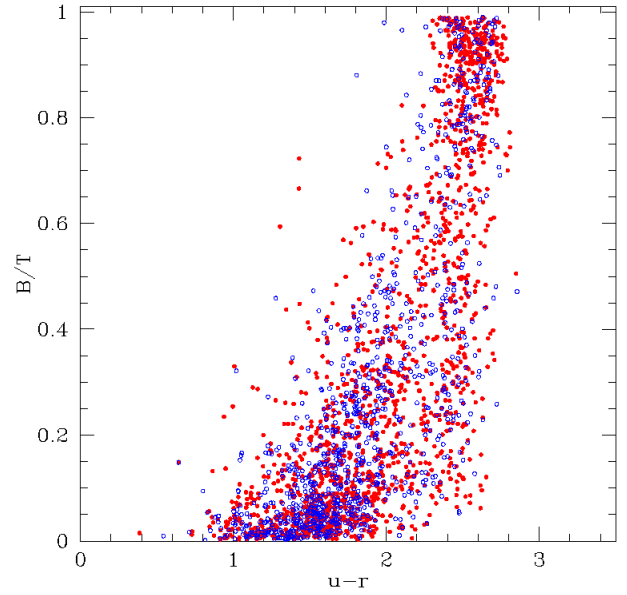


**Figure 14.**  $B/T$  ratios for the galaxies in voids as predicted by the Millennium Run (open circles). Note that, blue galaxies are disk dominated while red galaxies are bulge dominated. Red galaxies with  $u - r > 2.5$  have  $B/T$  ratios which suggest they are elliptical galaxies. For a comparison we show the same  $B/T$  ratios as a function of color for galaxies in the field (filled circles). Galaxies in voids are similar to that of the field.

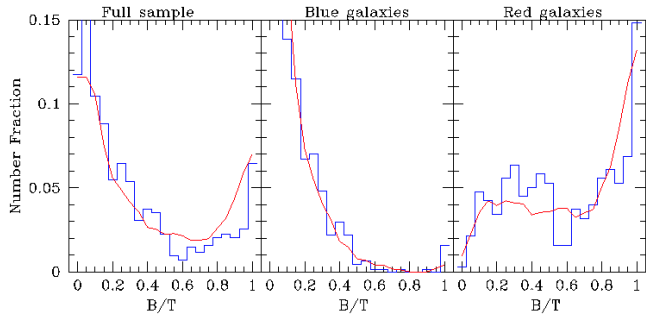


**Figure 15.**  $B/T$  distributions for the galaxies in voids (histograms) and field (curves) in the Millennium Run. Left panel: Full samples. Central Panel: Blue galaxies. Right panel: Red galaxies

are none in our voids, by definition. But the results suggest that, if anything, there may be an excess of redder galaxies in voids over what one might naively expect.

If one considers the blue and red galaxies separately, there does not appear to be any difference between void galaxies and the overall population of galaxies. Within the blue and red populations separately, the color distributions, morphology distributions (i.e. concentration and  $B/T$  ratios), and correlation of specific star formation rate with color appear nearly indistinguishable between void and non-void galaxies. A similar result has been found when galaxies are separated by their *local* environment by Balogh et al. (2004). These results suggest that the processes governing the star formation history, which determines the color and specific star formation rate, are largely independent of environment on any scale.

We compare our results with the latest predictions from state-of-the-art semi-analytic models using the Millennium Run galaxy catalog (Springel et al. 2005; Croton et al. 2005). The predictions from the Millennium Run qualitatively agree with the observed results. The number density profiles for Millennium are in very good agreement with those of the observations, showing the same trends. We do not see a density spike at the edges of voids when we look at the profiles either in real or redshift space.

In the Millennium run sample, as in the observed data, we see an excess of blue galaxies and a deficit of red galaxies in voids with respect to the overall galaxy population, but the effect is more extreme in the simulations than in the observed data. Within the blue population, the simulated galaxies appear identical inside and outside of voids, as we observe, but the red population appears to differ between void and non-void galaxies, in contrast to what we observe. For the specific star formation rates, we do not see any systematic differences between galaxies in voids and the general population. Still, the specific star formation rates seem more concentrated in galaxies with  $u-r$  color around 1.6. Analysis of the  $B/T$  relation for galaxies in the Millennium Run, again, does not show any systematic difference between galaxies in voids and the field. There are ellipticals in voids, still less than in the field.

## ACKNOWLEDGMENTS

We would like to thank Darren Croton, Charlie Conroy and Simon D.M. White for useful comments and discussions that helped to improve the manuscript. SGP, FP & JBR thank support from the Spanish MEC under grant PNAYA 2005-07789. AK and JH acknowledge support of the NSF grant AST-0407072. SGP and FP thank the Astronomy Department of NMSU for hospitality during their visits to NMSU.

The Millennium Run simulation used in this paper was carried out by the Virgo Supercomputing Consortium at the Computing Center of the Max-Planck Society in Garching.

Funding for the creation and distribution of the SDSS Archive has been provided by the Alfred P. Sloan Foundation, the Participating Institutions, the National Aeronautics and Space Administration, the National Science Foundation, the U.S. Department of Energy, the Japanese Monbukagakusho, and the Max Planck Society. The SDSS Web site is <http://www.sdss.org/>.

The SDSS is managed by the Astrophysical Research Consortium (ARC) for the Participating Institutions. The Participating Institutions are The University of Chicago, Fermilab, the Institute for Advanced Study, the Japan Participation Group, The Johns Hopkins University, the Korean Scientist Group, Los Alamos National Laboratory, the Max-Planck-Institute for Astronomy (MPIA), the Max-Planck-Institute for Astrophysics (MPA), New Mexico State University, University of Pittsburgh, University of Portsmouth, Princeton University, the United States Naval Observatory, and the University of Washington.

## REFERENCES

- Abazajian, K., et al. 2003, *AJ*, 126, 2081
- Baldry, I. K., et al. 2004, *ApJ*, 600, 681
- Benson, A. J., Hoyle, F., Torres, F., & Vogeley, M. S. 2003, *MNRAS*, 340, 160
- Balogh, M. L., et al. 2004, *ApJ*, 615, L101
- Bernardi, M., et al. 2003a, *AJ*, 125, 1849
- Blanton, M. R., et al. 2001, *ApJ*, 121, 2358
- Blanton, M. R., Lin, H., Lupton, R. H., Maley, F. M., Young, N., Zehavi, I., & Loveday, J. 2003a, *AJ*, 125, 2276
- Brinchmann, J., et al. 2004, *MNRAS*, 351, 1151
- Colberg, J. M., Sheth, R. K., Diaferio, A., Gao, L., & Yoshida, N. 2005, *MNRAS*, 360, 216
- Croton, D., et al. 2005, *MNRAS*, 356, 1155
- Dressler, A. 1980, *ApJ*, 236, 351
- Dressler, A., et al. 2004, *ApJ*, 617, 867
- Eisenstein, D. J., et al. 2001, *AJ*, 122, 2267
- Fukugita, M., Ichikawa, T., Gunn, J. E., Doi, M., Shimasaku, K., & Schneider, D. P. 1996, *AJ*, 111, 1748
- Grogin, N. A., & Geller, M. J. 2000, *ApJ*, 119, 32
- Gottlöber, S. et al. 2003, *MNRAS*, 344, 715
- Gunn, J. E., et al. 1998, *ApJ*, 116, 3040
- Hogg, D. W., et al. 2004, *ApJ*, 601, L29
- Kauffmann, G., et al. 2003, *MNRAS*, 341, 33
- Lupton, R. H., Gunn, J. E., & Szalay, A. S. 1999, *AJ*, 118, 1406
- MacArthur, L. A., Courteau, S., & Holtzman, J. A. 2003, *ApJ*, 582, 689
- Patiri, S. G., Betancort-Rijo, J., & Prada, F. 2006a, *MNRAS*, 368, 1132

- Patiri, S. G., Betancort-Rijo, J. E., Prada, F., Klypin, A. K. & Gottlöber, S. 2006b, MNRAS, 369, 335
- Pier, J. R., et al. 2003, AJ, 125, 1559
- Postman, M., & Geller, M. J. 1984, ApJ, 281, 95
- Rojas, R. R., Vogeley, M. S., Hoyle, F. & Brinkmann, J. 2004, ApJ, 617, 50
- Rojas, R. R., Vogeley, M. S., Hoyle, F. & Brinkmann, J. 2005, ApJ, 624, 571
- Scranton, R. et al. 2002, ApJS, 579, 48
- Sheth, R. & Tormen, G., 2002, MNRAS, 39, 61
- Springel, V. et al. 2005, *Nature*, 435, 629
- Stoughton, C. et al. 2002, AJ, 123, 485
- Strauss, M. A., et al. 2002, AJ, 124, 1810S
- Strateva, I., et al. 2001, ApJ, 122, 1874
- York, D. G. et al. 2000, AJ, 120, 1579